

# Performance Analysis of Distributed Space-Time Block Encoded Sensor Networks

Mischa Dohler, *Member, IEEE*, Yonghui Li, *Member, IEEE*, Branka Vucetic, *Fellow, IEEE*,  
A. Hamid Aghvami, *Fellow, IEEE*, Marylin Arndt, *Member, IEEE*, and Dominique Barthel

**Abstract**—Sensor networks are comprised of nodes with minimal processing and RF functionalities. In such networks, it is assumed that a source sensor communicates with a target sensor over a number of relaying sensors by utilising distributed but cooperative low-complexity space-time encoding techniques, thereby achieving highly robust communication links. Each relaying stage is hence comprised of a given number of cooperating sensor nodes which may or may not exchange additional data. The contribution of this paper is the derivation of throughput-maximising resource allocation strategies for various sensor network configurations. The case of full data exchange at each relaying stage is analysed first, which is then relaxed to the case of partial data exchange. Monte-Carlo simulations are used to numerically verify the theoretically derived performance of distributed sensor networks. It is shown that notable power savings can be achieved compared to traditional single link and non-optimised sensor networks.

*Index Terms*—

MIMO Systems, Distributed Information Systems, Sensor Networks

## I. INTRODUCTION

The function of sensors is to sense certain features of their surroundings and pass this information to a sensor or unit which is capable of processing such data. Sensor networks are significantly different from traditional ad-hoc networks. Firstly, the number of sensor nodes in a sensor network can be several orders of magnitude higher than the number of nodes in an ad-hoc network. Moreover, sensor nodes are usually densely deployed, prone to failures and limited in power provision, computational complexity and memory [1].

The majority of the sensors are stationary; however, some communication paths between them may potentially be permanently or frequently obstructed. That may effect the throughput and stability of the routing path from source to target sensor. It is therefore a task of a sensor network designer to allow for a robust data transmission with minimal power consumption and complexity. The aim of this paper is hence to analyse

and optimise the performance of sensor networks for below described topologies.

**Background.** To date, a considerable amount of work has been dedicated to the conceptual design, information and communication theoretic analysis and practical implementation of sensor networks and underlying communication paradigms.

As for practical demonstrations, worth mentioning are the landmark WINS [3] and SmartDust [4] projects which aimed to integrate sensing, computing, and wireless communication capabilities into a small form factor to enable low-cost production of tiny sensor nodes in large numbers [5]. In the meantime, innumerable other projects appeared which have aimed to investigate various practical issues related to a sensor network deployment; for example, France Télécom's participation in the IST EU project PULSERS have resulted in functioning sensor networks [6].

As for the conceptual proposition of communication topologies tailored to the requirements of sensor networks, most notable is the landmark contribution [1] which highlights prior art and research challenges. One of the major design constraints mentioned in [1] has been the requirement on low complexity and fairly high robustness, which triggered distributed and cooperative data relaying topologies to be applied to sensor networks. The process of data relaying, i.e. the transmission of data from source to destination via at least one intermediate node, is known to yield information theoretical gains [7]–[14] and also drastic power savings due to the nonlinear behaviour of the aggregate pathloss [15]. Simple cooperation between the relaying nodes is known to provide additional diversity and hence boost capacity and performance further, as demonstrated in [16]–[20]. Furthermore, the process of distributed and cooperative data processing abates the limitation of having only one antenna element per sensor [21]–[32], thereby factually creating a multiple-input-multiple-output (MIMO) channel and yielding associated capacity and performance gains [33]–[39].

Although the method of relaying has been introduced in 1971 by van der Meulen [7] and has also been studied in [8], a first rigorous information theoretical analysis of the relay channel has been exposed by Cover in [9], [10]. The capacity of such a simple three-terminal relaying configuration was shown to exceed the capacity of a direct link, where Gaussian communication channels only have been assumed. This work has been extended by [11], [23], where the information theoretically offered throughput per terminal in a large scale relaying network has been analysed. In [21], the information theoretical results for distributed space-time

Manuscript received March 9, 2004; revised August 26, 2005; accepted January 24, 2006.

M. Dohler, M. Arndt and D. Barthel are with France Télécom R&D, 28 Chemin du Vieux Chêne, 38243 Meylan Cedex, France (phone: +33-4-7676-4514, fax: +33-4-7676-4450, emails: {Mischa.Dohler, Marylin.Arndt, Dominique.Barthel}@francetelecom.com).

Y. Li and B. Vucetic are with School of Electrical and Information Engineering, University of Sydney, Australia (emails: {lyh, branka}@ee.usyd.edu.au).

A.H. Aghvami is with King's College London, Centre for Telecommunications Research, 26-29 Drury Lane, London WC2B 5RL, UK (email: hamid.aghvami@kcl.ac.uk).

channels with possible feedback have been utilised to design simple communication protocols taking into account systems with and without temporal diversity, as well as various forms of cooperation. It has been demonstrated that cooperation yields full spatial diversity, which allows drastic transmit power savings at the same level of outage probability for a given communication rate.

As for communication theoretical work, [16] has been a milestone contribution where a very simple but effective user cooperation protocol has been suggested to boost the uplink capacity and lower the uplink outage probability for a given rate. The simple cooperative protocol has been extended by the same authors to more sophisticated schemes, which can be found in the excellent contributions [17] and [18]. The contributions [25] are a conceptual and mathematical extension to [16], where energy-efficient multiple access protocols are suggested based on decode-and-forward and amplify-and-forward relaying technologies.

Error rate, throughput and other performance metrics of distributed cooperative relaying networks have been analysed in [40]–[50], [51]–[57], and [32]. The analysis in [52] facilitates asymptotic error rates of generic cooperative topologies to be characterised in closed-form. This analysis has then been extended in [54] to obtain the error rates of distributed space-time block encoded cooperative relaying systems, as well as algorithms which allocate optimum power to the relaying nodes under conditions different from this work.

**Contributions.** The contributions of this paper can be summarised as follows:

- 1) The symbol error rates over generalised Nakagami fading channels have been derived in closed form, where each subchannel may obey different statistics.
- 2) The asymptotic end-to-end bit error rates are derived in closed form for a generic distributed and cooperative relaying topology.
- 3) This facilitates low-complexity throughput maximising resource allocation strategies to be derived in closed form, where adaptation is performed on power, frame duration, and modulation index.
- 4) Finally, the performance of above developed strategies is assessed for a wide variety of sensor network topologies.

**Assumptions.** It is assumed that each sensor is in possession of one antenna element only, and the transceiver utilises a time division multiple access (TDMA) protocol. In TDMA, each sensor receives data over the entire frequency band  $W$  and a frame duration  $T_1$ . After a possible processing, the data is retransmitted over the entire frequency band  $W$  and in a frame duration  $T_2$ , during which time it is not capable of receiving any data.

It is also assumed that an appropriate medium access control is deployed, which guarantees that at any time only one transmission link from source to target sensor is active. It is also assumed that the protocol facilitates the exchange of some non-frequent control data between the sensors, e.g. the average channel gains in the network, synchronisation data, etc.

It is further assumed that spatially adjacent sensor are grouped such that they allow for a distributed MIMO reception and re-transmission. Since the sensors are spatially separated,

no correlation will be observed. Sensors belonging to the same relaying stage may or may not exchange additional data among each other. Note that the choice of grouping is beyond this paper; however, the exposed analysis can certainly aid the design of optimum grouping and cooperation strategies.

Note that the TDMA protocol does not allow immediate relaying of the data stream, i.e. the data has to be downconverted to baseband, amplified, stored and upconverted before retransmission. To save memory, a hard decision is performed on the data stream prior to storage, the complexity and power consumption of which is negligible compared to the other processes. Furthermore, the load/store operations are known to consume a non-negligible amount of power, which is mainly due to the fairly high capacitance of the data buses [58], [59]. To minimise the amount of load/store operations in a sensor, baseband data processing ought to be avoided where possible; this includes operations like channel coding, cyclic redundancy check (CRC), etc.

To reflect the cheap and low-complexity hardware architecture of sensor nodes, above mentioned reasons stipulate the deployment of regenerative relaying and the decision on the correctness of a received packet to be drawn at the target processing unit only.

The aim of the analysis is to optimise the throughput for a given total transmission power in dependency of the prevailing average channel conditions. All, be they slowly changing or constant, average channel gains of the topology are assumed to be available within each sensor node, as they can be measured once or at low duty cycles.

**Paper Structure.** In Section II, the system model is described in detail. The principle of a distributed (sensor) network is explained, as is the encoding/decoding strategy at each sensor. In Section III, the error rates of distributed space-time block codes are exposed. These are then utilised in Sections IV and V to derive throughput-maximising resource allocation strategies assuming full and partial cooperation at each relaying stage, respectively. Finally, conclusions are drawn in Section VI.

## II. SYSTEM MODEL

### A. General Deployment

The subsequent description relates to a generalised deployment of distributed and cooperative space-time block encoded multistage sensor networks, as depicted in Figure 1. Here, a source sensor (s-S) communicates with a target unit or target sensor (t-S) via a given number of relaying sensors (r-Ss). Spatially adjacent r-Ss are grouped into Virtual Antenna Arrays (VAAs), thereby forming a cooperative relaying VAA (r-VAA) tier. The s-S and t-S themselves might be a member of a VAA, henceforth referred to as source VAA (s-VAA) and target VAA (t-VAA), respectively. The coordinated process of data relaying from the same tier is referred to as *cooperation* or *cooperative communication* [21], whereas the process of data relaying within the same tier is referred to as *data exchange*.

For the sake of generality, sensor nodes of the same tier are allowed to exchange data, thereby further boosting the network performance. It is understood that this might be a too complex

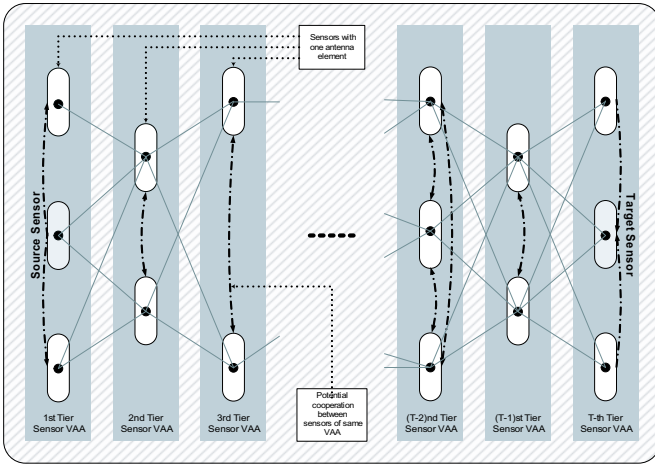


Fig. 1. Multi-stage distributed and cooperative sensor network.

process for sensor nodes of current hardware configuration; however, it might be applicable to future sensor networks or to current ad hoc networks.

The s-S, t-S and r-Ss possess only one antenna element, depicted as a large dot in Figure 1. Furthermore, the sensors may or may not exchange data among each other within the same VAA tier. The cooperative link is shown as a dash-dotted line. Each r-S of the same r-VAA transmits the prior agreed spatial branch of a space-time block codeword, where the encoding is based on the received and detected symbol from the previous r-VAA tier. The hence created MIMO sub-channels are shown as solid lines.

Clearly, the exchange of data within a relaying tier yields a higher throughput; however, at the expense of additional complexity, relaying power and frame duration when operating in TDMA. The latter two are assumed to be negligible in the current analysis. This is asymptotically justified because the proximity of the sensors belonging to the same stage allows establishing near error-free links with a higher modulation order (hence short frame duration) and lower power (compared to the transmission power from stage to stage).

It is further assumed that during communication from the s-S to the t-S no interference occurs among the stages. The resource allocation strategies have therefore to guarantee that fractional frame durations are allocated to each relaying stage in an orthogonal manner [32].

### B. Distributed Space-Time Block Encoding and Decoding

**Source Sensor.** The s-S Gray-maps  $b_0$  source information bits onto symbol  $x$  by utilising an  $M_0$ -PSK or  $M_0$ -QAM signal constellation, where  $b_0 = \log_2 M_0$ . The data stream is broadcasted to the adjacent sensors.

**First Tier Relaying Sensors (s-VAA).** The broadcasted data is received by the r-Ss belonging to the first tier VAA. They detect the data, space-time encode it and transmit it simultaneously with a total power  $S_1$  over an allocated fractional frame duration  $T_1$ . Each r-S Gray-maps  $s_1 b_1$  bits onto symbols  $x_1, x_2, \dots, x_{s_1}$  by utilising an  $M_1$ -PSK or  $M_1$ -QAM signal constellation, where  $b_1 = \log_2 M_1$  and  $s_1$  is the

number of symbols per space-time encoding. The  $\{x_k\}_{k=1}^{s_1}$  are encoded with an orthogonal space-time coding matrix  $\mathcal{G}_1$  of size  $d_1 \times t_1$ , where  $d_1$  is the number of symbol durations required to transmit the space-time codeword, and  $t_1$  is the number of distributed r-Ss (and therefore equivalent to the actual number of transmit antennas). At each time instant  $k$ , the encoded symbols  $c_{k,i}$  with  $k = 1, \dots, d_1$  and  $i = 1, \dots, t_1$  are transmitted simultaneously from the  $i^{th}$  distributed r-S. Clearly, the rate of the first tier space-time block code is  $R_1 = s_1/d_1$ .

**Second Tier Relaying Sensors.** The second relaying tier is formed by  $q_2$  spatially adjacent sensors, with one antenna each. Some sensors may exchange received data among each other, thereby forming  $Q_2$  clusters, where  $1 \leq Q_2 \leq q_2$ . The case of  $Q_2 = 1$  represents the scenario where all sensors cooperate, whereas  $Q_2 = q_2$  means that none of the sensors cooperate. The  $j^{th}$  cluster is assumed to consist of  $r_{2,j}$  sensors thereby achieving  $r_{2,j}$  receive antennas, where  $1 \leq j \leq Q_2$  and  $q_2 = \sum_{j=1}^{Q_2} r_{2,j}$ . Therefore,  $Q_2$  space-time block encoded MIMO channels are created, each with  $t_1$  transmit antennas and  $r_{2,j \in (1, Q_2)}$  receive antennas.

After data exchange, the data is space-time block decoded and re-encoded according to a given orthogonal space-time coding matrix  $\mathcal{G}_2$  of size  $d_2 \times t_2$  with a rate of  $R_2$ , where the encoding and transmission process is the same as described above. The number of transmit elements  $t_2$  is at most the number of sensors  $q_2$  in the second tier.

**T<sup>th</sup> Tier Relaying Sensors (t-VAA).** The de-coding/encoding process is continued until the VAA with the t-S is reached. The sensors in the T-th tier receive data from the previous tier. They relay the data to the target sensor.

**Target Sensor.** The t-S receives and space-time block decodes the data, after which it performs the final detection. If the s-S deploys a channel code, e.g. a simple trellis code, then the t-S performs the equivalent channel decoding (which has not been considered in this paper).

Each relaying sensor tier clearly may use a different signal constellation and STBC, i.e. it may adapt its modulation in dependency of the prevailing channel conditions. It is only of importance that the consecutive tier has knowledge of the transmission parameters of the previous tier.

## III. ERROR RATES OF DISTRIBUTED STBCS

The derivation of the fractional resource allocation strategies relies on the error rates of the space-time block codes (STBCs), where the sub-channel gains from any transmit to any receive sensor node may vary. This is in contrast to traditional MIMO systems, where the sub-channel gains are assumed to be equal. Therefore, the bit error rates (BERs), symbol error rates (SERs) and frame error rates (FERs) for distributed STBCs over Rayleigh and Nakagami flat fading channels with different channel statistics are given here. Note that the BERs and FERs are easily obtained from the SERs at high SNRs.

### A. Symbol Error Rates

The space-time encoding and decoding scheme, as depicted in Figure 2, represents an arbitrary stage within the multi-stage

$$P_{\text{PSK}}(e) = \frac{1}{\left(1 + \frac{g_{\text{PSK}} \gamma S}{R t N}\right)^u} \left[ \frac{1}{2\sqrt{\pi}} \frac{\Gamma(u+1/2)}{\Gamma(u+1)} {}_2F_1\left(u, 1/2; u+1; \left(1 + \frac{g_{\text{PSK}} \gamma S}{R t N}\right)^{-1}\right) + \frac{\sqrt{1-g_{\text{PSK}}}}{\pi} F_1\left(1/2, u, 1/2-u; 3/2; \frac{1-g_{\text{PSK}}}{1 + \frac{g_{\text{PSK}} \gamma S}{R t N}}, 1-g_{\text{PSK}}\right) \right] \quad (1)$$

$$P_{\text{QAM}}(e) = \frac{1}{\left(1 + \frac{g_{\text{QAM}} \gamma S}{R t N}\right)^u} \frac{2q}{\sqrt{\pi}} \frac{\Gamma(u+1/2)}{\Gamma(u+1)} {}_2F_1\left(u, 1/2; u+1; \left(1 + \frac{g_{\text{QAM}} \gamma S}{R t N}\right)^{-1}\right) - \frac{1}{\left(1 + 2\frac{g_{\text{QAM}} \gamma S}{R t N}\right)^u} \frac{2q^2}{\pi(2u+1)} F_1\left(1, u, 1; u+3/2; \frac{1 + \frac{g_{\text{QAM}} \gamma S}{R t N}}{1 + 2\frac{g_{\text{QAM}} \gamma S}{R t N}}, 1/2\right) \quad (2)$$

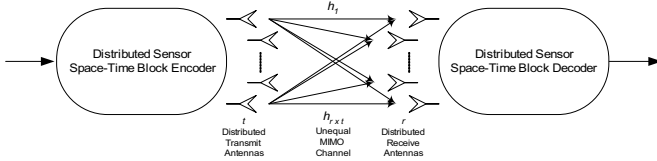


Fig. 2. Distributed space-time block code transceiver model.

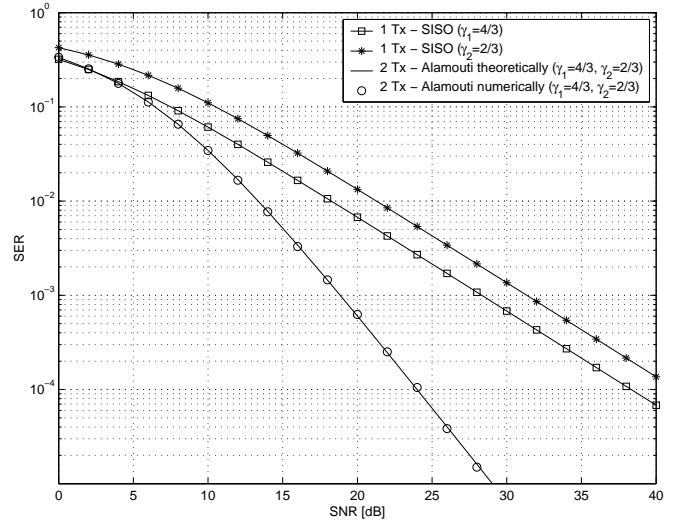
sensor network introduced before. Here, a STBC of rate  $R$  is transmitted from a transmitter with  $t$  transmit elements and received by  $r$  receive elements. The flat fading sub-channel from the  $i$ -th transmit element to the  $j$ -th receive element is denoted as  $h_{(i-1)r+j}$ , where  $1 \leq i \leq t$  and  $1 \leq j \leq r$ . The  $u \triangleq t \times r$  sub-channels have an average power  $\gamma_{(i-1)r+j} \triangleq E\{|h_{(i-1)r+j}|^2\}$ , where  $E\{\cdot\}$  denotes the expectation.

**Rayleigh Fading - Equal Sub-Channel Gains.** According to [60], the SER for M-PSK over a MIMO channel with equal sub-channel gains  $\gamma_1 = \dots = \gamma_u \triangleq \gamma$  can be expressed in closed form as given in (1), where  $g_{\text{PSK}} \triangleq \sin^2(\pi/M)$ ,  $M$  is the modulation order,  $\Gamma(x)$  is the complete Gamma function,  ${}_2F_1(a, b; c; x)$  is the Gauss hypergeometric function with 2 parameters of type 1 and 1 parameter of type 2 [61] (§9.14.1), and the function  $F_1(a, b, b'; c; x, y)$  is the Appell hypergeometric function of two variables [61] (§9.180.1). To simplify notation, eq. (1) is denoted as  $P_{\text{PSK}}(e) = P_{\text{PSK}}(u, t, R, \gamma, S/N, M)$ . Similarly, the SER of M-QAM can be expressed as given in (2), where  $g_{\text{QAM}} \triangleq 3/2/(M-1)$  and  $q \triangleq 1 - 1/\sqrt{M}$ . To simplify notation in subsequent analysis, the notation  $P_{\text{QAM}}(e) = P_{\text{QAM}}(u, t, R, \gamma, S/N, M)$  is adopted.

**Rayleigh Fading - Unequal Sub-Channel Gains.** For unequal sub-channel gains, the SERs of M-PSK and M-QAM modulation schemes have been derived in [32] as

$$P_{\text{PSK/QAM}}(e) = \sum_{i=1}^u K_i \cdot P_{\text{PSK/QAM}}(1, t, R, \gamma_i, S/N, M) \quad (3)$$

where the constants  $K_i$  are given as  $K_i = \prod_{i'=1, i' \neq i}^u \gamma_i / (\gamma_i - \gamma_{i'})$ . As an example, Figure 3 depicts the SER versus the SNR in dB for the distributed Alamouti scheme with one receive antenna only. The power of the unequal channel coefficients is arbitrary chosen such that  $\gamma_1 = 4/3$  and  $\gamma_2 = 2/3$ . The cases are depicted where


 Fig. 3. SER versus SNR for a distributed Alamouti system operating at 2 bits/s/Hz with  $\gamma_1 = 4/3$  and  $\gamma_2 = 2/3$ .

only the channel with power  $\gamma_1$  is utilised, and where only the channel with power  $\gamma_2$  is utilised, and where the distributed Alamouti STBC is utilised. The latter is corroborated by numerical simulations.

Clearly, the distributed scenario provides diversity gain even for unbalanced channel gains, whereas the single links exhibit a less steep error curve. The gain of the distributed case at a SER of  $10^{-5}$  is approximately 20dB.

**Rayleigh Fading - Generic Sub-Channel Gains.** Generally, the channel gains  $\gamma_{i \in (1, u)}$  can be different where some gains are repeated. There shall be  $g \leq u$  distinct channel gains, which are henceforth referred to as  $\hat{\gamma}_{i \in (1, g)}$  with each of them being repeated  $\nu_{i \in (1, g)}$  times. In this case, the respective error rates can be expressed as [32]

$$P_{\text{PSK/QAM}}(e) = \sum_{i=1}^g \sum_{j=1}^{\nu_i} K_{i,j} \cdot P_{\text{PSK/QAM}}(j, t, R, \hat{\gamma}_i, S/N, M) \quad (4)$$

where coefficients  $K_{i,j}$  are expressed as

$$K_{i,j} = \frac{1}{(\nu_i - j)! \left(-\frac{1}{R} \frac{\hat{\gamma}_i S}{t N}\right)^{\nu_i - j}} \times \frac{\partial^{\nu_i - j}}{\partial s^{\nu_i - j}} \left[ \prod_{\substack{i'=1, \\ i' \neq i}}^g \frac{1}{\left(1 - \frac{1}{R} \frac{\hat{\gamma}_{i'} S}{t N} \cdot s\right)^{\nu_{i'}}} \right]_{s=\left(\frac{1}{R} \frac{\hat{\gamma}_i S}{t N}\right)^{-1}} \quad (5)$$

**Nakagami Fading - Equal Sub-Channel Gains.** The cases of Nakagami fading are similarly derived as for the Rayleigh fading cases. Assuming a Nakagami fading channel with equal sub-channel gains  $\gamma_1 = \dots = \gamma_u \triangleq \gamma$  and equal fading parameters  $f_1 = \dots = f_u \triangleq f$ , the respective SERs can be obtained as [32]

$$P_{\text{PSK/QAM}}(e) = P_{\text{PSK/QAM}}(fu, ft, R, \gamma, S/N, M). \quad (6)$$

**Nakagami Fading - Unequal Sub-Channel Gains.** Finally, the respective error rates for a Nakagami fading channel with different sub-channel gains  $\gamma_{i \in (1,u)}$  and different fading factors  $f_{i \in (1,u)}$  can be expressed as [32]

$$P_{\text{PSK/QAM}}(e) = \sum_{i=1}^u \sum_{j=1}^{f_i} K_{i,j} \cdot P_{\text{PSK/QAM}}(j, jt, R, \gamma_i, S/N, M) \quad (7)$$

where

$$K_{i,j} = \frac{1}{(f_i - j)! \left(-\frac{1}{R} \frac{\gamma_i S}{f_i t N}\right)^{f_i - j}} \times \frac{\partial^{f_i - j}}{\partial s^{f_i - j}} \left[ \prod_{\substack{i'=1, \\ i' \neq i}}^u \frac{1}{\left(1 - \frac{1}{R} \frac{\gamma_{i'} S}{f_{i'} t N} \cdot s\right)^{f_{i'}}} \right]_{s=\left(\frac{1}{R} \frac{\gamma_i S}{f_i t N}\right)^{-1}} \quad (8)$$

### B. Bit Error Rates

The derived dependencies relate the average transmitted signal power to the SER. The exact BER of generic M-PSK and M-QAM schemes, however, is difficult to obtain. Analysis is greatly simplified if the bits are Gray-mapped onto the symbol, i.e. adjacent symbol constellation points differ only by one bit [62]. In that case, the BER  $P_b(e)$  is easily related to the SER via [62]

$$P_b(e) = \frac{P_s(e)}{\log_2(M)} \quad (9)$$

at low error rates or sufficiently high SNRs.

### C. Packet Error Rates

A data packet is assumed to consist of  $B$  bits. A packet error occurs if at least one of the  $B$  bits is in error. With the assumptions of Section I, the bits in a packet are independent from each other which yields for the PER

$$P_p(e) = 1 - (1 - P_b(e))^B \quad (10a)$$

$$= 1 - B P_b(e) \quad (10b)$$

where (10b) holds at low FERs or sufficiently high SNRs. Note that in the case of slow fading channels, eqs. (10) can be approached with the aid of a suitable time interleaver.

## IV. MAXIMUM THROUGHPUT FOR FULL DATA EXCHANGE

The error rates obtained in the previous section are utilised here to derive fractional resource allocation rules assuming that a decision on the correctness of the received data packet is done at the target processing unit. This should not be confused with transparent relaying, where the information is amplified and forwarded. It is also in contrast to a stage-by-stage detection, where a decision on the correctness of the received packet is done at each sensor relaying stage.

If all relaying sensors per stage exchange the received data and this takes places at a sufficiently high SNR, then the signal samples from the previous stage are the same at all relaying sensors. Therefore, if an error occurs in the signal from the previous stage, then that error is the same in all relaying sensors belonging to the same stage. This applies not only to STBCs, but to any type of applied space-time coding.

Such a scenario provides a great simplification to analysis, since the errors in consecutive stages become independent. This is in contrast to a generic relaying process with no or partial data exchange (clustering), where one relaying cluster may have a more reliable estimate than another relaying cluster in the same relaying tier VAA, leading to error-dependencies between the stages.

Subsequently, the problem of maximising the end-to-end throughput is shown to be equivalent to the problem of minimising the end-to-end BER. For the sake of clarity, the fractional resource allocation rules are derived for the cases of full data exchange in this section first, and for no or partial data exchange in the subsequent section.

### A. Problem Simplification

It is assumed here that the source sensor (s-S) transmits  $B$  bits per frame to the target sensor (t-S) via  $K = T - 1$  relaying stages. The normalised end-to-end throughput in [bits/s/Hz] from s-S to t-S can be expressed as

$$\Theta = \min_{v \in (1,K)} \{ \alpha'_v R_v \log_2(M_v) \} \cdot (1 - P_{p,e2e}(e)) \quad (11)$$

where  $\alpha'_v$ ,  $R_v$  and  $M_v$  are the fractional frame duration, STBC rate and modulation index of the  $v^{\text{th}}$  stage respectively,  $P_{f,e2e}(e)$  is the end-to-end FER, and  $1 \leq v \leq K$ .

Eq. (11) has to be understood as follows. If there were no losses between a directly communicating s-S and t-S, then all of the  $B$  bits reach the receiver; the throughput normalised by the total number of sent bits hence mounts to 1. The use of a modulation scheme with index  $M$  and a STBC with rate  $R$  during a fractional frame duration  $\alpha'$  to accomplish such link results in a throughput, normalised by the utilised time and bandwidth, as  $1 \cdot \alpha' \cdot R \cdot \log_2(M)$  [bits/s/Hz]. For a communication system with  $K$  relaying stages, the weakest link in the chain determines the throughput, hence  $\min_{v \in (1,K)} \{ \alpha'_v R_v \log_2(M_v) \}$ . Since the decision on the correctness of a data packet is done at the target processing unit and not in the relaying nodes, the term is further diminished by the loss caused by the end-to-end PER  $P_{p,e2e}(e)$ . It is thus the aim to derive optimum resource allocation strategies, which maximise the end-to-end throughput.

To this end, note that  $P_{p,e2e}(e)$  is a function of the error rates occurring in each relaying stage and hence depends on  $M_{v \in (1,K)}$ ,  $R_{v \in (1,K)}$  and the fractional transmission power allocated to each stage. Optimising (11) with respect to these parameters is very complex, which is the reason why the optimisation process is performed in three stages.

First, the modulation indices  $M_{v \in (1,K)}$  are fixed (which is relaxed in the third optimisation stage) and the asymptotic case where  $\text{SNR} \rightarrow \infty$  is considered. This reduces (11) to

$$\Theta = \min_{v \in (1,K)} \left\{ \alpha'_v R_v \log_2(M_v) \right\} \quad (12)$$

where the fractional frame durations  $\alpha'_v$  need to be chosen such as to maximise  $\Theta$  under constraint  $\sum_{v=1}^K \alpha'_v = 1$ . This is achieved by equating all  $\alpha'_v R_v \log_2(M_v)$  which results in

$$\alpha'_v = \frac{\prod_{w=1, w \neq v}^K R_w \cdot \log_2(M_w)}{\sum_{k=1}^K \prod_{w=1, w \neq k}^K R_w \cdot \log_2(M_w)}. \quad (13)$$

Second, the throughput in (11) is maximised if the end-to-end PER is minimised. With reference to (10b), this is clearly achieved by minimising the end-to-end BER  $P_{b,e2e}(e)$ , which requires optimum fractional transmission power to be assigned to each relaying stage. The BER at each stage is related with the occurring SER via (9), where for low error rates one symbol error causes one bit error.

Third, the optimum modulation order  $M_{v \in (1,K)}$  has to be determined in dependency of the previously derived fractional resource allocations. This is easily done by permuting all possible modulation orders at each stage such as to maximise the end-to-end throughput. Since the number of modulation orders will be limited, such optimisation is feasible at low computational complexity.

Subsequently, the second step is performed assuming either total or partial (clustered) data exchange in each stage. The near-optimum fractional power allocation rules are first derived, then assessed in terms of their precision; finally, the maximum achievable throughput will be illustrated by means of a few examples.

### B. Resource Allocation Strategy

Under the assumption of full data exchange, each of the  $K$  relaying stages experiences independent BERs, here denoted as  $P_{b,v \in (1,K)}(e)$ , caused by independent SERs  $P_{s,v \in (1,K)}(e)$ . A bit from the s-S is received correctly at the t-S only when at all stages the bit has been transmitted correctly (the probability that two or more wrong bits may result again in a correct bit is approaching zero for sufficiently high SNRs). The end-to-end BER can therefore be expressed as

$$P_{b,e2e}(e) = 1 - \prod_{v=1}^K (1 - P_{b,v}(e)) \quad (14)$$

which, at low BERs or sufficiently high SNRs at every stage, can be written as

$$P_{b,e2e}(e) = \sum_{v=1}^K P_{b,v}(e) \quad (15)$$

$$= \sum_{v=1}^K \frac{P_{s,v}(e)}{\log_2(M_v)} \quad (16)$$

where  $M_v$  is the modulation order at the  $v^{\text{th}}$  stage. Further analysis concentrates on the case of Rayleigh fading with equal channel gains per relaying stage; other cases are a straightforward extension to the exposed analysis, utilising the expressions developed Section III. Assuming that each stage is allocated a fractional power  $\beta'_v$ , the above-given dependency can be expressed as

$$P_{b,e2e}(e) = \sum_{v=1}^K \frac{P_{s,v}(u_v, t_v, R_v, \gamma_v, \beta'_v \cdot S/N, M_v)}{\log_2(M_v)} \quad (17)$$

where the SERs  $P_{s,v}(\cdot) = P_{\text{PSK/QAM}}(\cdot)$  are given through (1) and (2), respectively. Furthermore,  $u_v \triangleq t_v \cdot r_v$ ,  $t_v$  and  $r_v$  are the number of transmit and receive antennas in the  $v^{\text{th}}$  stage,  $R_v$  is the rate of the STBC,  $\gamma_v$  is the average attenuation experienced,  $S$  is the total power allowed to deliver the information from source to sink, and  $N$  is the noise power.

The optimisation process has only to be performed with respect to the fractional power allocation  $\beta'_{v \in (1,K)}$ . Even so, the optimisation process is very intricate. To simplify analysis further, an upper bound to the derived SERs for M-PSK and M-QAM is invoked. Following the analysis outlined in [63, chapter 9], the SER for M-PSK in the  $v^{\text{th}}$  relaying stage can be upper-bounded as

$$P_{s,v}(e) \leq \frac{\frac{M_v-1}{M_v}}{\left(1 + \beta'_v \frac{g_{\text{PSK},v} \gamma_v S}{R_v t_v N}\right)^{u_v}} \quad (18)$$

where  $g_{\text{PSK},v} = \sin^2(\pi/M_v)$ . The end-to-end BER for an M-PSK scheme can hence be upper-bounded as

$$P_{b,e2e}(e) \leq \sum_{v=1}^K \frac{M_v-1}{M_v \log_2(M_v)} \left(1 + \beta'_v \frac{g_{\text{PSK},v} \gamma_v S}{R_v t_v N}\right)^{-u_v} \quad (19)$$

Following a similar approach, the upper-bound for the end-to-end BER of an M-QAM scheme can be derived as

$$P_{b,e2e}(e) \leq \sum_{v=1}^K \frac{2q_v}{\log_2(M_v)} \left[ \left(1 + \beta'_v \frac{g_{\text{QAM},v} \gamma_v S}{R_v t_v N}\right)^{-u_v} + \frac{q_v}{2} \left(1 + 2\beta'_v \frac{g_{\text{QAM},v} \gamma_v S}{R_v t_v N}\right)^{-u_v} \right] \quad (20)$$

$$\approx \sum_{v=1}^K \frac{2q_v}{\log_2(M_v)} \left(1 + \beta'_v \frac{g_{\text{QAM},v} \gamma_v S}{R_v t_v N}\right)^{-u_v} \quad (21)$$

where  $g_{\text{QAM},v} = 3/2/(M_v - 1)$  and  $q_v = 1 - 1/\sqrt{M_v}$ . Note that in (21) the second summand appearing in (20) was neglected due to  $q_v/2 < 1$  and  $(1 + 2x)^{-u_v}$  being much less than  $(1 + x)^{-u_v}$  for  $x$  sufficiently large and  $u_v \geq 1$ . Either modulation scheme results in an upper-bound unified below as

$$P_{b,e2e}(e) \leq \sum_{v=1}^K A_v (1 + B_v \beta'_v)^{-u_v} \quad (22)$$

The constants  $A_v$  and  $B_v$  are obtained by comparing (22) with (19) or (21) to arrive at

$$A_v = \begin{cases} \frac{M_v-1}{M_v \log_2(M_v)} & \text{for M-PSK} \\ \frac{2q_v}{\log_2(M_v)} & \text{for M-QAM} \end{cases} \quad (23)$$

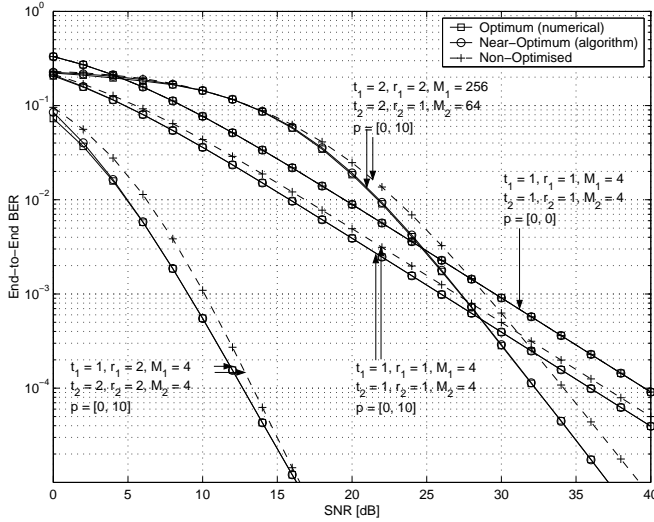


Fig. 4. Comparison between optimum and near-optimum, as well as non-optimised end-to-end BER for various configurations of a two-stage relaying network.

and

$$B_v = \begin{cases} \frac{g_{\text{PSK},v} \gamma_v S}{R_v t_v N} & \text{for M-PSK} \\ \frac{g_{\text{QAM},v} \gamma_v S}{R_v t_v N} & \text{for M-QAM} \end{cases} \quad (24)$$

From this it is shown in the Appendix (Derivation I) that the throughput-maximising fractional power allocations  $\beta'_{v \in (1,K)}$  have to obey

$$\beta'_v = \left[ \sum_{w=1}^K \alpha'_w \left( \frac{u_v^{-1} A_v^{-1} B_v^{u_v}}{u_w^{-1} A_w^{-1} B_w^{u_w}} \right)^{\frac{1}{u_{\max}+1}} \right]^{-1} \quad (25)$$

where  $u_{\max} = \max(u_1, \dots, u_K)$ .

### C. Performance of Algorithm

The performance of the developed algorithm is assessed by means of Figures 4–7 for M-QAM schemes only. Note that if reference is made to the non-optimised scenario, then only the fractional transmission power is meant not to be optimised since the frame duration is easily related to the modulation order. Note further that the obtained graphs are generally labelled on the parameter  $p$  defined as

$$p \triangleq \left[ 10 \log_{10} \left( \frac{\gamma_1}{\gamma_1} \right), 10 \log_{10} \left( \frac{\gamma_2}{\gamma_1} \right), \dots, 10 \log_{10} \left( \frac{\gamma_K}{\gamma_1} \right) \right]$$

which characterises the relative strength in dB of the  $K$  relaying stages with respect to the first stage.

Explicitly, Figure 4 depicts the end-to-end BER versus the SNR in the first link in dB for various 2-stage sensor networks deploying the developed fractional power allocation strategy (25), which is also compared against a numerically obtained optimum and a non-optimum allocation.

The first scenario, where  $t_{1,2} = r_{1,2} = 1$ ,  $M_{1,2} = 4$  (QPSK) and  $p = [0, 0]$  dB, is entirely symmetric which leads to the same performance for all three allocation strategies. The second scenario is the same as the first, with the only difference that the channel in the second stage is now 10 times stronger

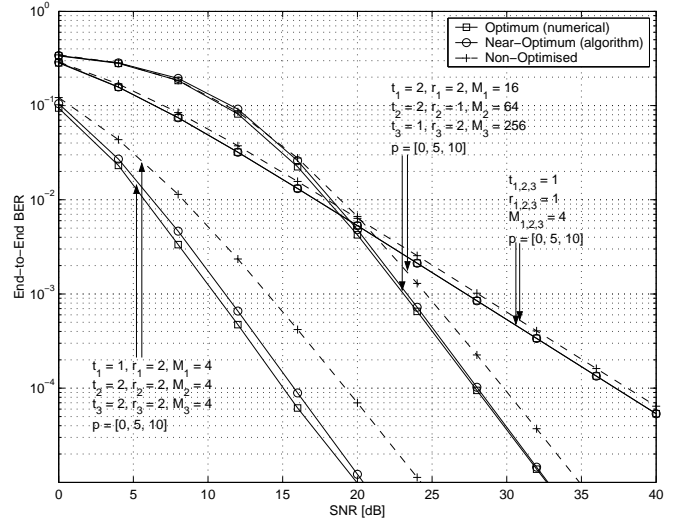


Fig. 5. Comparison between optimum and near-optimum, as well as non-optimised end-to-end BER for various configurations of a three-stage relaying network.

than in the first stage, i.e.  $p = [0, 10]$  dB. The thus created non-symmetric scenario reveals a performance difference between the optimised (solid lines) and non-optimised (dashed line) power allocation.

It can be observed that the optimum and developed allocation strategy yield the same performance for any of the depicted configurations. Furthermore, the gain of an optimised system over a non-optimised system is highest for very asymmetric cases, here for  $t_1 = 2, r_1 = 2, t_2 = 2, r_2 = 1, M_1 = 256, M_2 = 64$  and  $p = [0, 10]$  dB. At a target end-to-end BER of  $10^{-5}$ , about 1 dB in power can be saved.

Figure 5 is similar in its nature to Figure 4, with the only difference that a three-stage sensor network is scrutinised. Similar observations can be made for these scenarios, where gains of almost 4 dB can be observed. This corroborates the importance of the derived allocation strategy.

The throughput of a two-stage system is illustrated by means of Figure 6, which utilises the fractional resource allocation strategies (13) and (25). The system deployed has the number of bits fixed to  $B = 100$ ; furthermore, for all configurations  $M_{1,2} = 4$  (QPSK) and  $p = [0, 10]$  dB. It can be observed that in the region of low SNR, the developed allocation strategy performs worse than the optimum one. This is obvious, as the fractional frame durations have been derived assuming the SNR to be large.

For most of the transitional region from zero-throughput to maximum-throughput, however, the derived allocations yield near-optimum throughput. In contrast, no optimisation exhibits drastic losses in the transitional region. For example, given the scenario with  $t_{1,2} = r_{1,2} = 2$  operating at a normalised throughput of 0.5 bits/s/Hz, transmission power of 2 dB are lost which amounts to approximately 40%.

Observe also that the cases of full-rate STBC in each stage yield the same maximum throughput, whereas the case with the 3/4-rate STBC has a lower maximum throughput, notwithstanding the fact that it constitutes the strongest link. This is due to the limiting spectral efficiency of the STBC

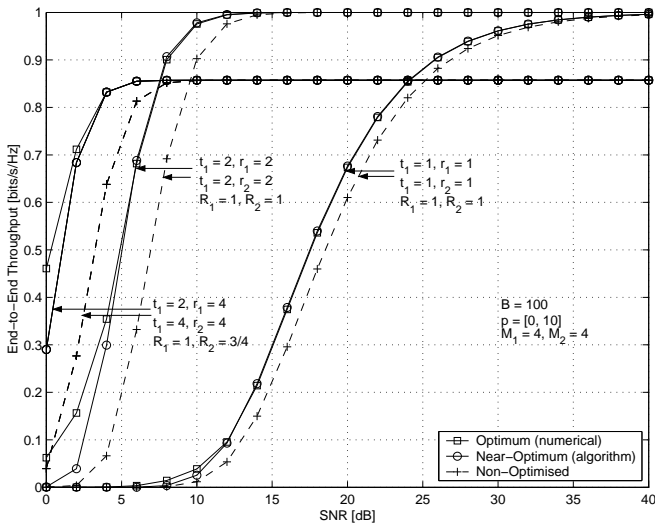


Fig. 6. Comparison between optimum and near-optimum, as well as non-optimised end-to-end throughput for various configurations of a two-stage relaying network.

with a rate less than one. Clearly, the strength of the link determines the rate with which the system approaches the limiting throughput for the  $\text{SNR} \rightarrow \infty$ .

The precision of the fractional allocation algorithm for fixed modulation indexes allows performing a final numerical optimisation in each relaying stage over all possible modulation indexes. The low complexity of (13) and (25) guarantees that such optimisation comes at little additional computational power.

Such numerical optimisation was performed for a 2-stage sensor network with  $p = [0, 10]\text{dB}$  and  $t_{1,2} = r_{1,2} = 2$ . Each stage could choose a modulation index belonging to the set  $M_{1,2} = (2, 4, 16, 64, 256)$ ; this leads to 25 possible combinations which are calculated in a fraction of a second. The performance gains in terms of decreased transmission power or increased throughput are clear from Figure 7, where the near-optimum adaptive modulation per stage is compared against various fixed combinations.

For example, if the sensor network was to operate at a normalised throughput of 2 bits/s/Hz, then the best but fixed modulation index consumes 20dB transmission power. The optimum selection, however, consumes only 15dB which yields a performance benefit of 33%.

### V. MAXIMUM THROUGHPUT FOR PARTIAL DATA EXCHANGE

Partial or no data exchange at each relaying stage results in parallel MIMO channels, all of possibly different strength. An example of such clustering process is depicted by means of Figure 8 with none of the relaying sensors per cooperative stage communicating with each other.

Here, the first stage spans two independent SISO channels with average attenuation  $\gamma_{1,1}$  and  $\gamma_{1,2}$ , respectively. Each of these channels causes independent BERs, denoted as  $P_{1,1}$  and  $P_{1,2}$ , respectively. Similarly, the second stage spans two independent MISO channels, where the first MISO channel

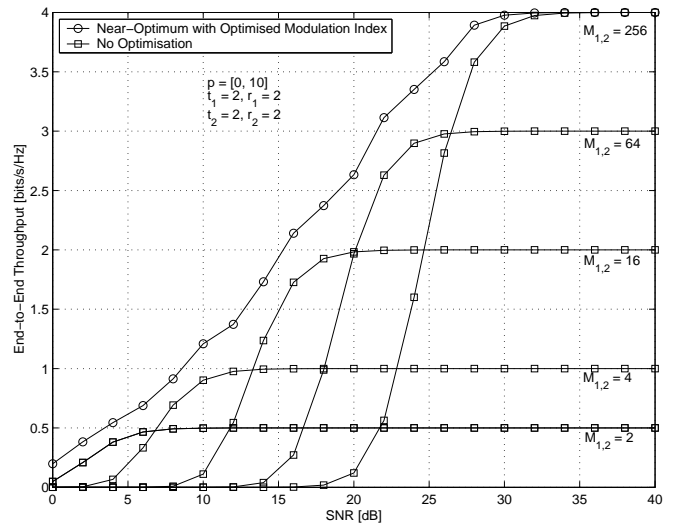


Fig. 7. Numerically optimised modulation index where  $M_{1,2} = (2, 4, 16, 64, 256)$  to yield near-optimum end-to-end throughput, compared to non-optimised systems.

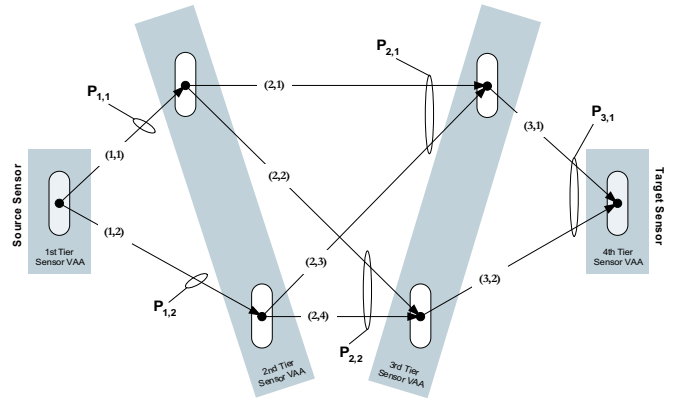


Fig. 8. 3-stage distributed sensor network without data exchange among sensors belonging to the same relaying stage.

consists of channels with average attenuations  $\gamma_{2,1}$  and  $\gamma_{2,3}$ , and the second MISO channel consists of channels with average attenuations  $\gamma_{2,2}$  and  $\gamma_{2,4}$ . Furthermore, assuming an error free input into the second VAA relaying tier, the BERs at the output of the MISO channels are  $P_{2,1}$  and  $P_{2,2}$ . Finally, the third stage spans a single MISO channel with a BER of  $P_{3,1}$ .

Note that the r-Ss belonging to the same stage need to transmit at the same rate; furthermore, they obviously need to know which part of the space-time block code to transmit, which could be negotiated at discovery or determined randomly. Furthermore, it is assumed that synchronisation among all sensors belonging to the same relaying stage is perfect. This is clearly an idealistic assumption; however, below analysis can serve as an upper bound on the performance of such networks. The interested reader is referred to [46] for an analysis of synchronisation errors.

To obtain the exact end-to-end BER is not trivial, because an error in the first stage may propagate to the t-S; however, it may also be corrected at the next stage. Referring to Figure 8,

$$\begin{aligned}
 P_{b,e2e}(e) = & \left[ P_{1,1}(e) \left( \frac{\gamma_{2,1}}{\gamma_{2,1} + \gamma_{2,3}} \frac{\gamma_{3,1}}{\gamma_{3,1} + \gamma_{3,2}} + \frac{\gamma_{2,2}}{\gamma_{2,2} + \gamma_{2,4}} \frac{\gamma_{3,2}}{\gamma_{3,1} + \gamma_{3,2}} \right) + \right. \\
 & \left. P_{1,2}(e) \left( \frac{\gamma_{2,4}}{\gamma_{2,2} + \gamma_{2,4}} \frac{\gamma_{3,2}}{\gamma_{3,1} + \gamma_{3,2}} + \frac{\gamma_{2,3}}{\gamma_{2,1} + \gamma_{2,3}} \frac{\gamma_{3,1}}{\gamma_{3,1} + \gamma_{3,2}} \right) \right] + \\
 & \left[ P_{2,1}(e) \left( \frac{\gamma_{3,1}}{\gamma_{3,1} + \gamma_{3,2}} \right) + P_{2,2}(e) \left( \frac{\gamma_{3,2}}{\gamma_{3,1} + \gamma_{3,2}} \right) \right] + \left[ P_{3,1}(e) \right]
 \end{aligned} \quad (26)$$

for example, it is assumed that the same information bit is erroneously received over the link denoted as (1,1) and correctly for (1,2). Then, the STBC formed by (2,1) and (2,3) has as its input one erroneous and one correct information bit. Assuming that  $\gamma_{2,3} \gg \gamma_{2,1}$ , then the error does not further propagate since it will be outweighed by the correct bit. Alternatively, if  $\gamma_{2,3} \ll \gamma_{2,1}$ , then there is a large likelihood that the error propagates.

This creates dependencies between the error events at each stage in dependency of the modulation scheme used, the prevailing channel statistics, the average channel attenuations, as well as the STBC chosen. The fairly complex interdependencies become tractable under asymptotic conditions as outlined below.

Generally, it is desirable to develop an approach which decouples the error events at the respective stages. To this end, it is assumed that the system operates at low error rates or sufficiently high SNRs, which causes only one error event at a time in the entire sensor network. This is a realistic assumption, because one would design a network yielding near error free communication.

Let us assume that an error occurs in link (1,1); however, (1,2) is error free. Then the probability that the error propagates further is related to the strengths of channels (2,1) and (2,3). The elegant asymptotic error rate analysis developed in [52] and further extended to distributed space-time block codes in [54] shows that the probability of such error to propagate is asymptotically proportional to the strength (i.e. first order channel statistics) of the STBC branch it departs from; here, (2,1) for one of two MISO channels, and (2,2) for the other one.

Therefore, the probability that an error, which occurred in link (1,1) with probability  $P_{1,1}$ , propagates through the MISO channel spanned by (2,1) and (2,3) is given as  $P_{1,1} \cdot \gamma_{2,1}/(\gamma_{2,1} + \gamma_{2,3})$ , where the strength of the erroneous channel (2,1) is normalised by the total strength of both sub-channels. To capture the probability that such an error propagates until the t-S, all possible paths in the network have to be found and the original probability of error weighed with the ratios between the respective path gains.

Taking the above-said into account and assuming that at high SNRs only one such error will occur at any link, the end-to-end BER for the network depicted in Figure 8 can be

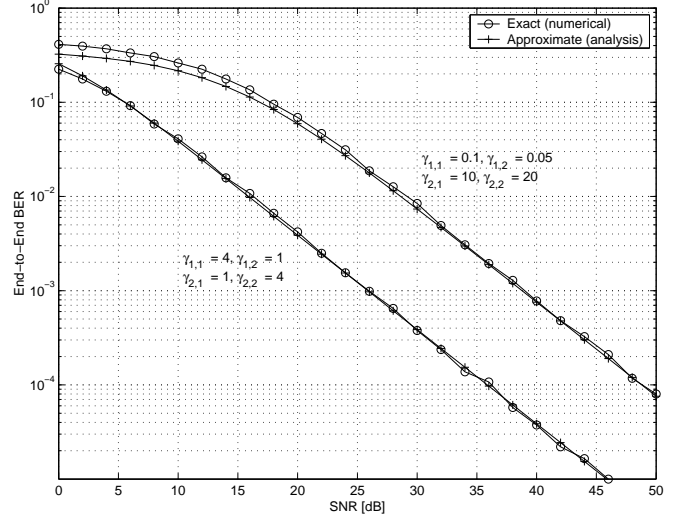


Fig. 9. Numerically obtained and derived end-to-end BER versus the SNR in the first link for a two-stage network without data exchange.

expressed as given in (26). This can be simplified to

$$\begin{aligned}
 P_{b,e2e}(e) = & \left[ \xi_{1,1} P_{1,1}(e) + \xi_{1,2} P_{1,2}(e) \right] + \\
 & \left[ \xi_{2,1} P_{2,1}(e) + \xi_{2,2} P_{2,2}(e) \right] + \\
 & \left[ \xi_{3,1} P_{3,1}(e) \right]
 \end{aligned} \quad (27)$$

where  $\xi_{v,i}$  is the probability that an error occurring in link  $(v,i)$  will propagate to the t-S. This result is easily generalised to sensor networks of any size and any form of partial data exchange. To this end, remember that there are  $Q_{v \in (1,K)}$  data exchanging clusters at the  $v^{th}$  stage, each of which will yield an error probability of  $P_{v \in (1,K), i \in (1, Q_v)}$ . The asymptotic end-to-end BER is hence given as

$$P_{b,e2e}(e) = \sum_{v=1}^K \sum_{i=1}^{Q_v} \xi_{v,i} P_{v,i}(e), \quad (28)$$

where the probabilities  $\xi_{v,i}$  are determined by the specific network topology. The BERs  $P_{v,i}(e)$  can be found from (9) and any of the previously derived SERs with an appropriate number of transmit and receive antennas per cluster, as well as prevailing channel conditions. The applicability of the derived end-to-end BER is assessed by means of Figures 9 and 10.

Explicitly, Figure 9 compares the numerically obtained and the derived end-to-end BER versus the SNR in the first link for

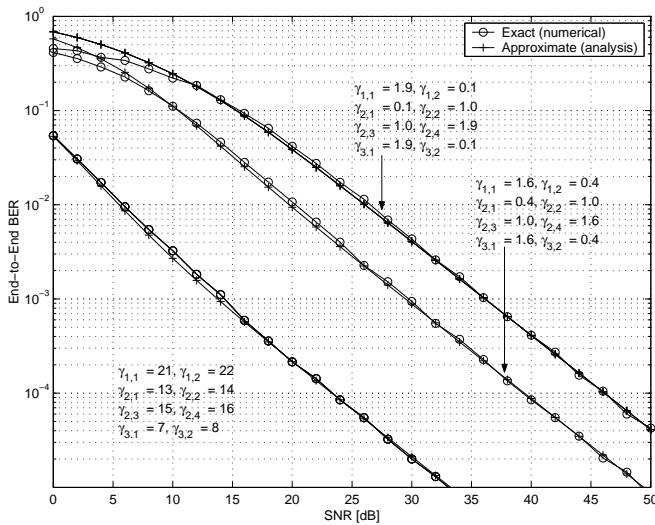


Fig. 10. Numerically obtained and derived end-to-end BER versus the SNR in the first link for a three-stage network without data exchange.

a two-stage network as depicted in Figure 8 without the second stage. For all simulations, QPSK has been used. The graphs are labelled on the respectively utilised channel gains. It can be observed that the derived BER differs from the exact one for low SNRs; however, for an increasing SNR, both curves converge.

Figure 10 compares the numerically obtained and the derived end-to-end BER versus the SNR in the first link for a three-stage network as depicted in Figure 8. The curves are again labelled on the channel gains. From Figure 10 it is clear that the derived end-to-end BER holds with high precision for a variety of different scenarios.

The derived end-to-end BERs in form of (28) allow one to assign optimum fractional powers  $\beta'_{v \in (1,K)}$  such that, together with the fractional frame durations  $\alpha'_{v \in (1,K)}$ , near-optimum end-to-end throughput is achieved. The fractional frame durations are clearly independent of the channel statistics or the choice of clustering in the high SNR mode; therefore, eq. (13) for  $\alpha'_{v \in (1,K)}$  holds true. The fractional power allocations are derived as follows.

Without loss of generality, let us assume that all links obey Rayleigh fading and have a different channel gain. The error rates are then governed by (3), where  $u$  has to be replaced by the number of sub-channels created in each of the  $Q_v$  clusters. The fractional power allocations are derived in the Appendix (Derivation II) as

$$\beta'_v = \left[ \sum_{w=1}^K \alpha'_w \sqrt{\frac{\sum_{i=1}^{Q_v} \sum_{j \in i} \xi_{v,i}^{-1} K_{v,i,j}^{-1} A_v^{-1} B_{v,i,j}}{\sum_{i=1}^{Q_w} \sum_{j \in i} \xi_{w,i}^{-1} K_{w,i,j}^{-1} A_w^{-1} B_{w,i,j}}} \right]^{-1} \quad (29)$$

where the notation  $j \in i$  represents the  $j^{\text{th}}$  sub-channel belonging to the  $i^{\text{th}}$  cluster. The partial expansion coefficients

$K_{v,i,j}$  in the  $v^{\text{th}}$  stage for the  $i^{\text{th}}$  cluster can be written as

$$K_{v,i,j} = \prod_{j' \in i, j' \neq j} \frac{\gamma_{v,j}}{\gamma_{v,j} - \gamma_{v,j'}} \quad (30)$$

which has  $u_{v,i}$  multiplicative terms. The constant  $A_v$  is given by (23), whereas

$$B_{v,i,j} = \begin{cases} \frac{g_{\text{PSK},v} \gamma_{v,j \in i} S}{R_v t_v N} & \text{for M-PSK} \\ \frac{g_{\text{QAM},v} \gamma_{v,j \in i} S}{R_v t_v N} & \text{for M-QAM} \end{cases} \quad (31)$$

The throughput is similarly obtained as for the case of full cooperation, and is hence not further illustrated here.

## VI. CONCLUSIONS

The performance of distributed multi-stage sensor networks has been analysed in terms of error rates, achievable throughput and attainable power savings when compared to traditional non-distributed networks. It has been assumed that a source sensor communicates with a target processing unit or target sensor via relaying sensors, where each sensor is attributed only one antenna element. Furthermore, spatially adjacent relaying sensors have been grouped into Virtual Antenna Arrays (VAAs). The thereby accomplished distributed MIMO relaying channels allow low-complexity space-time block codes (STBCs) to be deployed at each relaying stage. The performance of such sensor network topology has been analysed in three steps.

First, the error rates of STBCs over Rayleigh and Nakagami flat fading channels with arbitrary channel gains and fading statistics have been given.

Second, the error rates have then been utilised to derive throughput-maximising fractional resource allocation algorithms, assuming full data exchange among the sensors belonging to the same relaying stage. The fractional power and frame duration allocations have been determined which maximise the end-to-end data throughput or, alternatively, minimise the required transmission power.

Third, the analysis has then been extended to the case of no or partial data exchange at each relaying stage. Examples have demonstrated the advantageous applicability of the derived strategies, where transmit power savings of up to 40% have been observed. Also, an asymptotic expression for the end-to-end error rates in the case of partial data exchange at each relaying stage has been obtained.

The transmission process is known to consume between 30%-50% of the power in a sensor node [64]. Savings of up to 40% transmission power, facilitated by the herein derived allocation algorithms, hence yield a significant overall power savings.

Finally, it should be noted that the analysis exposed in this paper is equally applicable to general ad-hoc type networks with deployed space-time block coding. If complexity is not the limiting factor, then distributed space-time trellis codes can be deployed and analysed similarly to space-time block codes.

## APPENDIX

**Derivation I.** To prove (25), eq. (22) is rearranged as shown in (32), where the constraints  $\sum_{v=1}^K \alpha'_v \beta'_v = 1$  for a TDMA-based relaying system have been used [32]. Without loss

$$\begin{aligned}
 P_{b,e2e}(e) &\leq \frac{A_1}{(1+B_1\beta'_1)^{u_1}} + \sum_{v=2}^K \frac{A_v}{(1+B_v\beta'_v)^{u_v}} = \frac{A_1}{\left(1+\alpha'_1{}^{-1}B_1\alpha'_1\beta'_1\right)^{u_1}} + \sum_{v=2}^K \frac{A_v}{(1+B_v\beta'_v)^{u_v}} \\
 &= \frac{A_1}{\left(1+\alpha'_1{}^{-1}B_1\left(1-\sum_{v=2}^K\alpha'_v\beta'_v\right)\right)^{u_1}} + \sum_{v=2}^K \frac{A_v}{\left(1+B_v\beta'_v\right)^{u_v}}
 \end{aligned} \tag{32}$$

$$\frac{u_1 A_1 \alpha'_1{}^{-1} B_1}{\left(1+\alpha'_1{}^{-1}B_1\left(1-\sum_{v=2}^K\alpha'_v\beta'_v\right)\right)^{u_1+1}} = \frac{u_2 A_2 B_2}{\left(1+B_2\beta'_2\right)^{u_2+1}} \tag{33}$$

$$\begin{aligned}
 &\vdots \\
 &= \frac{u_K A_K B_K}{\left(1+B_K\beta'_K\right)^{u_K+1}}
 \end{aligned} \tag{34}$$

$$\frac{\alpha'_1{}^{-u_1} B_1^{u_1}}{u_1 A_1} \left(1-\sum_{v=2}^K\alpha'_v\beta'_v\right)^{u_1+1} = \frac{B_K^{u_K}}{u_K A_K} (\beta'_K)^{u_K+1} \tag{35}$$

$$\frac{B_2^{u_2}}{u_2 A_2} (\beta'_2)^{u_2+1} = \frac{B_K^{u_K}}{u_K A_K} (\beta'_K)^{u_K+1} \tag{36}$$

$$\begin{aligned}
 &\vdots \\
 \frac{B_{K-1}^{u_{K-1}}}{u_{K-1} A_{K-1}} (\beta'_{K-1})^{u_{K-1}+1} &= \frac{B_K^{u_K}}{u_K A_K} (\beta'_K)^{u_K+1}
 \end{aligned} \tag{37}$$

$$\alpha'_1{}^{-1} \left(\frac{B_1^{u_1}}{u_1 A_1}\right)^{\frac{1}{u_{\max}+1}} \left(1-\sum_{v=2}^K\alpha'_v\beta'_v\right) \approx \left(\frac{B_K^{u_K}}{u_K A_K}\right)^{\frac{1}{u_{\max}+1}} (\beta'_K) \tag{38}$$

$$\left(\frac{B_2^{u_2}}{u_2 A_2}\right)^{\frac{1}{u_{\max}+1}} (\beta'_2) \approx \left(\frac{B_K^{u_K}}{u_K A_K}\right)^{\frac{1}{u_{\max}+1}} (\beta'_K) \tag{39}$$

$$\begin{aligned}
 &\vdots \\
 \left(\frac{B_{K-1}^{u_{K-1}}}{u_{K-1} A_{K-1}}\right)^{\frac{1}{u_{\max}+1}} (\beta'_{K-1}) &\approx \left(\frac{B_K^{u_K}}{u_K A_K}\right)^{\frac{1}{u_{\max}+1}} (\beta'_K)
 \end{aligned} \tag{40}$$

of generality, the fractional power allocation  $\beta'_K$  for the last relaying stage will be derived. To obtain the optimum fractional power allocations which yield a minimum end-to-end BER, eq. (32) is differentiated  $K-1$  times along  $\beta_{v \in (2, K)}$ .

The obtained  $K-1$  equations are equated to zero to arrive at (33)–(34). For low target SERs,  $B_v\beta'_v \gg 1$  for any  $v \in (1, K)$ , which allows rearranging (33)–(34) to (35)–(37). This set of equations is difficult to resolve in closed form w.r.t. any of the  $\beta'_{v \in (1, K)}$ . To this end, the  $(u_{\max}+1)$ -st square root is taken of eqs. (35)–(37), where per definition  $u_{\max} = \max(u_1, \dots, u_K)$ . The choice of  $u_{\max}$  is motivated by the fact that the error in approximating  $(\beta'_v)^y$  by  $\beta'_v$  for  $0 < \beta'_v < 1$  and  $y \leq 1$  is smaller compared to the case when  $y > 1$ . Since such approximation is vital in further steps, it has to be made sure that the approximation error for the above equations is minimised. This justifies the choice of  $u_{\max}$ , as

it guarantees that  $y = (u_v+1)/(u_{\max}+1) \leq 1$  for any  $v \in (1, K)$ . Eqs. (35)–(37) can hence be recast into (38)–(40), which are easily resolved in favour of  $\beta'_2, \dots, \beta'_K$ , i.e.

$$\beta'_2 \approx \beta'_K \left(\frac{u_K^{-1} A_K^{-1} B_K^{u_K}}{u_2^{-1} A_2^{-1} B_2^{u_2}}\right)^{\frac{1}{u_{\max}+1}} \tag{41}$$

$\vdots$

$$\beta'_{K-1} \approx \beta'_K \left(\frac{u_K^{-1} A_K^{-1} B_K^{u_K}}{u_{K-1}^{-1} A_{K-1}^{-1} B_{K-1}^{u_{K-1}}}\right)^{\frac{1}{u_{\max}+1}} \tag{42}$$

which, when inserted into (38), yields

$$\beta'_K \cdot \sum_{v=1}^K \alpha'_v \left(\frac{u_K^{-1} A_K^{-1} B_K^{u_K}}{u_v^{-1} A_v^{-1} B_v^{u_v}}\right)^{\frac{1}{u_{\max}+1}} = 1 \tag{43}$$

where  $\beta'_K$  is now obtained and shown to be equivalent to (21)

for  $v = K$ . Other coefficients are similarly obtained. This concludes the proof.

**Derivation II.** To prove (29), recall that the asymptotic end-to-end BER is given as

$$P_{b,e2e}(e) = \sum_{v=1}^K \sum_{i=1}^{Q_v} \xi_{v,i} P_{v,i}(e) \quad (44)$$

where the weights  $\xi_{v,i}$  are derived in dependency of the network topology. With reference to (3), the BER of the  $i^{th}$  cluster in the  $v^{th}$  stage can be expressed as

$$P_{v,i}(e) = \sum_{j \in i} K_{v,i,j} \cdot P_{PSK/QAM}(1, t_v, R_v, \gamma_{v,j}, S/N, M_v) \quad (45)$$

where the expansion coefficients are given in (30). With reference to the analysis exposed in Section IV-B, it can be upper-bounded as

$$P_{v,i}(e) \leq \sum_{j \in i} \frac{K_{v,i,j} A_v}{1 + B_{v,i,j} \beta'_v}, \quad (46)$$

where the coefficients  $A_v$  are given by (23) and  $B_{v,i,j}$  by (31). Inserting (46) into (44) yields

$$P_{b,e2e}(e) \leq \sum_{v=1}^K \sum_{i=1}^{Q_v} \sum_{j \in i} \frac{\xi_{v,i} K_{v,i,j} A_v}{1 + B_{v,i,j} \beta'_v}. \quad (47)$$

The same procedure is now followed as already outlined in Derivation I, where (32) is extended by the additional sums; furthermore,  $A_v$  is replaced by  $\xi_{v,i} K_{v,i,j} A_v$  and  $u_v$  by 1, which finally yields (29).

REFERENCES

[1] I.F. Akyildiz, W. Su, Y. Sankarasubramaniam, E. Cayirci, "A survey on sensor networks," *IEEE Communications Magazine*, vol. 40 Issue: 8, Aug. 2002 pp. 102-114.  
 [2] R.C. Shah and J. Rabaey, "Energy Aware Routing for Low Energy Ad Hoc Sensor Networks", *IEEE Wireless Communications and Networking Conference (WCNC)*, March 17-21, 2002, Orlando, FL.  
 [3] Wireless Integrated Network Sensors, University of California, Los Angeles. Available: <http://www.janet.ucla.edu/WINS>  
 [4] J.M. Kahn, R.H. Katz, and K.S.J. Pister, "Next century challenges: Mobile networking for smart dust," *Proc. Mobicom*, 1999, pp. 483-492.  
 [5] V. Raghunathan, C. Schurgers, S. Park, and M. B. Srivastava, "Energy Aware Wireless Microsensor Networks", *IEEE Signal Processing*, March 2002.  
 [6] W. Hirt, D. Porcino, "Pervasive Ultra-wideband Low Spectral Energy Radio Systems (PULSERS)," *7th WWRF Meeting*, WWRF/WG4/UWB-Subgroup, Eindhoven, The Netherlands, Dec. 3-4, 2002.  
 [7] E. van der Meulen, "Three-terminal communication channels," *Adv. Appl. Prob.*, vol. 3, pp. 120-154, 1971.  
 [8] H. Sato, "Information transmission through a channel with relay," The Aloha System, University of Hawaii, Honolulu, Tech. Rep. B76-7, March 1976.  
 [9] T. Cover, A.A. El Gamal, "Capacity Theorems for the Relay Channel," *IEEE Trans. on Inform. Theory*, vol. IT-25, no. 5, pp.572-584, September 1979.  
 [10] T. Cover, J.A. Thomas, *Elements of Information Theory*, John Wiley & Sons, Inc., 1991.  
 [11] P. Gupta, P.R. Kumar, "The Capacity of Wireless Networks," *IEEE Trans. on Inform. Theory*, vol. 46, no. 2, pp. 388-404, March 2000.  
 [12] B. Schein, R. Gallager, "The gaussian parallel relay network," *Proc. Intl. Symp. on Info. Theory*, June 2000, p. 22.  
 [13] A. Host-Madsen, "On the capacity of wireless relaying," *Proc. of Vehicular Technology Conf.*, Sept. 2002, pp. 13337.

[14] A. Reznik, S. Kulkarni, and S. Verdu, "Capacity and Optimal Resource Allocation in the Degraded Gaussian Relay Channel with Multiple Relays," *Proc. Allerton Conf. Communications, Control, and Computing*, (Monticello, IL), Oct. 2002.  
 [15] T. J. Harrold, A. R. Nix, "Capacity Enhancement Using Intelligent Relaying For Future Personal Communications System", *Proceedings of VTC-2000 Fall*, pp. 2115-2120.  
 [16] A. Sendonaris, E. Erkip, B. Aazhang, "Increasing Uplink Capacity via User Cooperation Diversity," *Proc. IEEE ISIT*, p. 196, August 1998.  
 [17] A. Sendonaris, E. Erkip, B. Aazhang, "User Cooperation Diversity - Part I: System Description," *IEEE Transactions on Communications*, vol. 51, no. 11, November 2003, pp. 1927-1938.  
 [18] A. Sendonaris, E. Erkip, B. Aazhang, "User Cooperation Diversity - Part II: Implementation Aspects and Performance Analysis," *IEEE Transactions on Communications*, vol. 51, no. 11, November 2003, pp. 1939-1948.  
 [19] J.N. Laneman, G.W. Wornell, "Energy-efficient antenna sharing and relaying for wireless networks," *IEEE WCNC*, September 2000, Conference CD-ROM.  
 [20] T. E. Hunter and A. Nosratinia, Cooperation Diversity through Coding, in *Proc. IEEE Int. Symp. Information Theory (ISIT)*, (Lausanne, Switzerland), p. 220, July 2002.  
 [21] J.N. Laneman, *Cooperative Diversity in Wireless Networks: Algorithms and Architectures*, PhD Dissertation, MIT September 2002.  
 [22] P. Gupta, P. R. Kumar, "Towards and Information Theory of Large Networks: An Achievable Rate Region," *Proc. IEEE Int. Symp. Information Theory (ISIT)*, (Washington DC), p. 150, June 2001.  
 [23] P. Gupta, P.R. Kumar, "Towards an Information Theory of Large Networks: An Achievable Rate Region," *IEEE Trans. on Inform. Theory*, vol. 49, pp. 1877-1894, August 2003.  
 [24] A. Stefanov, E. Erkip, "Cooperative Space-Time Coding for Wireless Networks," *Proc. IEEE ITW*, pp. 50-53, April 2003.  
 [25] J. N. Laneman, D. N. C. Tse, G. W. Wornell, "Cooperative Diversity in Wireless Networks: Efficient Protocols and Outage Behavior," *IEEE Trans. Inform. Theory*, accepted for publication.  
 [26] J. N. Laneman, G. W. Wornell, "Distributed Space-Time Coded Protocols for Exploiting Cooperative Diversity in Wireless Networks," *IEEE Trans. Inform. Theory*, vol. 49, pp. 2415-2525, Oct. 2003.  
 [27] Y. Tang, M.C. Valenti, "Coded transmit macrodiversity: Block space-time codes over distributed antennas," *Proc. IEEE Vehicular Tech. Conf. (VTC)*, (Rhodes, Greece), May 2001, pp. 1435-1438.  
 [28] A. Stefanov, E. Erkip, "On the performance analysis of cooperative space-time coded systems" *Wireless Communications and Networking, WCNC 2003*, March 2003, Vol. 2, pp. 729-734.  
 [29] P.A. Anghel, G. Leus, M. Kavehl, "Multi-user space-time coding in cooperative networks," *Acoustics, Speech, and Signal Processing 2003*, April, 2003, vol. 4, pp 73-6.  
 [30] Y. Hua, Y. Mei, Y. Chang, "Wireless antennas making wireless communications perform like wireline communications," *IEEE Topical Conference on Wireless Communication Technology*, pp. 1-27, Honolulu, Hawaii, Oct 15-17, 2003.  
 [31] M. Dohler, F. Said, A. Ghorashi, H. Aghvami, "Improvements in or Relating to Electronic Data Communication Systems", Publication No. WO 03/003672, priority date 28 June 2001.  
 [32] M. Dohler, *Virtual Antenna Arrays*, PhD Thesis, King's College London, University of London, London, 2003.  
 [33] E. Telatar, "Capacity of multi-antenna Gaussian channels," *European Trans. on Telecomm.*, vol. 10, no. 6, pp. 585-595, Nov./Dec. 1999.  
 [34] G.J. Foschini and M.J. Gans, "On limits of wireless communications in a fading environment when using multiple antennas", *Wireless Personal Communications*, vol. 6, pp. 311-335, 1998.  
 [35] S.M. Alamouti, "A simple transmit diversity technique for wireless communications," *IEEE J-SAC*, vol. 16, No. 8, Oct. 1998.  
 [36] V. Tarokh, H. Jafarkhani, A. Calderbank, "Space-Time Block Codes from Orthogonal Design", *IEEE Trans. Inform. Theory*, Vol 45, No. 5, July 1999, pp. 1456-1466.  
 [37] V. Tarokh, H. Jafarkhani, and A.R. Calderbank, "Space-time block coding for wireless communications: Performance results", *IEEE Journal on selected areas in communications*, vol. 17, No. 3, Mar. 1999, pp. 451-460.  
 [38] V. Tarokh, N. Seshadri, A.R. Calderbank, "Space Time Codes for high data rate wireless communication: performance criterion and code construction," *IEEE Trans. Inform. Theory*, Vol 44, No. 2, March 1998, pp. 744-765.  
 [39] G.J. Foschini, "Layered Space-Time Architecture for Wireless Communication in a Fading Environment When Using Multi-Element Antennas"

- nas", *Bell Labs Technical Journal*, Vol. 1, No. 2, Autumn 1996, pp 41-59.
- [40] H. El Gamal, D Aktas, "Distributed space-time filtering for cooperative wireless networks," *IEEE GLOBECOM 03*, Vol. 4, Dec., 2003, pp. 1826-1830.
- [41] Mi-Kyung Oh, Xiaoli Ma, G.B. Giannakis, Dong-Jo Park, "Cooperative synchronization and channel estimation in wireless sensor networks," *Signals, Systems and Computers Conference 2003*, Vol. 1, Nov., 2003, pp. 238-242.
- [42] Shuguang Cui, A.J. Goldsmith, A. Bahai, "Energy-efficiency of MIMO and cooperative MIMO techniques in sensor networks," *IEEE Journal on Selected Areas in Communications*, Vol. 22, Issue 6, Aug. 2004, pp. 1089-1098.
- [43] S.K. Jayaweera, "An energy-efficient virtual MIMO architecture based on V-BLAST processing for distributed wireless sensor networks," *Sensor and Ad Hoc Communications and Networks 2004*, Oct., 2004, pp. 299-308.
- [44] Liang Xiao, Ming Xiao, "A new energy-efficient MIMO-sensor network architecture M-SENMA," *IEEE VTC2004-Fall*, vol. 4, Sept., 2004, pp. 2941-2945.
- [45] Wenyu Liu, Xiaohua Li, Mo Chen, "Energy Efficiency of MIMO Transmissions in Wireless Sensor Networks with Diversity and Multiplexing Gains," *Acoustics, Speech, and Signal Processing 2005*, March, 2005, pp. 897-900.
- [46] S. Jagannathan, H. Aghajan, A. Goldsmith, "The effect of time synchronization errors on the performance of cooperative MISO systems," *Global Telecommunications Conference Workshops 2004*, Nov./Dec., 2004, pp. 102-107.
- [47] J. Burdin, J. Duniak, "Cohesion of wireless sensor networks with MIMO communications," *IEEE SoutheastCon 2005*, April, 2005, pp. 547-551.
- [48] P. Mitran, H. Ochiari, V. Tarokh, "Space-time diversity enhancements using collaborative communications," *IEEE Transaction on Information Theory*, Vol. 51, Issue 6, June, 2005, pp. 2041-2057.
- [49] Wenqing Chen, Yong Yuan, Changchun Xu, Kezhong Liu, Zongkai Yang, "Virtual MIMO Protocol Based on Clustering for Wireless Sensor Network Computers and Communications 2005," *IEEE Symposium on ISCC 2005*, June, 2005, pp. 335-340.
- [50] S.K. Jayaweera, M.L. Chebolu, "Virtual MIMO and distributed signal processing for sensor networks - an integrated approach," *IEEE ICC 2005*, Vol. 2, May, 2005, pp. 1214-1218.
- [51] M.O. Hasna, M.-S. Alouini, "Outage probability of multihop transmission over nakagami fading channels," *IEEE Communications Letters*, vol. 7, no. 5, pp. 2168, 2003.
- [52] A. Ribeiro, X. Cai, G.B. Giannakis, "Symbol error probabilities for general cooperative links," *Proc. of Intl. Conf. on Communications*, June 20-24, 2004, pp. 3369-73.
- [53] P.A. Anghel, G. Leus, M. Kaveh, "Distributed space-time coding in cooperative networks," *Proc. of Intl. Conf. on Acoustics, Speech and Signal Proc.*, April, 2003, vol.4, pp. 73-6.
- [54] P.A. Anghel, M. Kaveh, "On the performance of distributed space-time coding systems with one and two non-regenerative relays," *IEEE Transactions on Wireless Communications*, to appear in 2005.
- [55] P.A. Anghel, M. Kaveh, "Exact symbol error probability of a cooperative network in a Rayleigh fading environment," *IEEE Transactions on Wireless Communications*, vol. 3, no. 5, pp. 141622, Sept. 2004.
- [56] Y. Hua, Y. Mei, Y. Chang, "Parallel wireless mobile relays with space-time modulations," *Proc. of IEEE Workshop on Statistical Signal Proc.*, St. Louis, MO, Sept. 2003.
- [57] Y. Chang and Y. Hua, "Diversity analysis of orthogonal space-time modulation for distributed wireless relays," *Intl. Conf. on Acoustics, Speech, and Signal Proc.*, Montreal, Canada, May 2004, vol. vol.4, pp. 5614.
- [58] V. Ekanayake, C. Kelly, R. Manohar, "An ultra low-power processor for sensor networks," *Architectural support for programming languages and operating systems*, Boston, MA, USA, pp. 27-36, 2004.
- [59] STM, "Data Sheet M72DW64000B," October 2003, p. 12, table 5.
- [60] H. Shin and J.H. Lee, "Exact symbol error probability of orthogonal space-time block codes," *Proc. of the IEEE Globecom*, Taipei, Taiwan, Nov. 17-21, pp.1547-1552, 2002.
- [61] I.S. Gradshteyn, I.M. Ryzhik, *Table of Integrals, Series, and Products*, Academia Press, sixth edition, 2000.
- [62] J. Proakis, *Digital communications*, McGraw Hill, Third edition, 1995.
- [63] M.K. Simon, M.-S. Alouini, *Digital Communication over Fading Channels*, John Wiley & Sons, Inc., Wiley Series in Telecommunications and Signal Processing, 2000.
- [64] C. Schurgers, V. Tsiatsis, S. Ganeriwal, M. Srivastava, "Optimizing Sensor Networks in the Energy-Latency-Density Design Space," *IEEE Trans on Mobile Computing*, vol. 1, no. 1, January-March 2002, pp. 70-80.

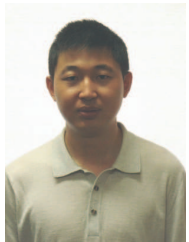


**Mischa Dohler** obtained his MSc degree in Telecommunications from King's College London in 1999, his Diploma in Electrical Engineering from Dresden University of Technology, Germany, in 2000, and his PhD from King's College London in 2003. He has been lecturer at the Centre for Telecommunications Research, King's College London, until June 2005. He is now in the R&D department of France Telecom working on embedded and future communication systems, such as opportunistic radio, cognitive radio, and wireless sensor networks.

Prior to Telecommunications, he studied Physics in Moscow. He has won various competitions in Mathematics and Physics, and participated in the 3rd round of the International Physics Olympics for Germany. He is a member of the IEEE and he has been the Student Representative of the IEEE UKRI Section, member of the Student Activity Committee of IEEE Region 8 and the London Technology Network Business Fellow for King's College London. He has published over 50 technical journal and conference papers, holds several patents, co-edited and contributed to several books, and has given numerous international short-courses. He has been TPC member and co-chair of various conferences and is member of the editorial board of the EURASIP journal.



**A. Hamid Aghvami** joined the academic staff at King's College, London in 1984. In 1989 he was promoted to Reader and Professor in Telecommunications Engineering in 1992. He is presently the Director of the Centre for Telecommunications Research at King's. Professor Aghvami carries out consulting work on Digital Radio Communications Systems for both British and International companies. He has published over 300 technical papers and given invited talks all over the world on various aspects of Personal and Mobile Radio Communications as well as giving courses on the subject worldwide. He was Visiting Professor at NTT Radio Communication Systems Laboratories in 1990 and Senior Research Fellow at BT Laboratories in 1998-1999. He is currently Executive Advisor to Wireless Facilities Inc., USA and Managing Director of Wireless Multimedia Communications LTD (his own consultancy company). He leads an active research team working on numerous mobile and personal communications projects for third and fourth generation systems, these projects are supported both by the government and industry. He is a distinguished lecturer and a member of the Board of Governors of the IEEE Communications Society. He has been member, Chairman, Vice-Chairman of the technical programme and organising committees of a large number of international conferences. He is also founder of the International Conference on Personal Indoor and Mobile Radio Communications (PIMRC). He is a fellow of the Royal Academy of Engineering, IEE and IEEE.



**Yonghui Li** (M'04) received his PhD degree in Electronic Engineering in November 2002 from Beijing University of Aeronautics and Astronautics and his PhD thesis has been awarded "best PhD thesis award." From 1999 - 2003, he was affiliated with Linkair Communication Inc, where he served as a project manager. Since 2003, he has been a research fellow in Telecommunication Lab, University of Sydney, Australia. His current research interests lie in the area of communications and include MIMO, multiple user communications, coding techniques

and wireless sensor networks. He has been involved in the technical committee of several international conferences, such as ICC'05, PIMRC'05, Wireless-Com'05 and so on.



**Marylin Arndt** is research group leader at FTRD research center in Meylan, France, in the area of Integration of Radio Application. She has graduated as an engineer from the "Ecole Nationale Supérieure de Télécommunications", Paris, and obtained her PhD in microelectronics from the University of Languedoc at Montpellier (1982). In 1982, she started at CNET (France Telecom Circuits Design Laboratory, Microelectronics Technologies Division) as an Audio Digital Signal Processing ASIC Designer, Baseband ASIC Designer, and DSP architecture designer.

In 1996, she commenced with France Telecom R&D, Telecom Circuits and Systems Laboratory, as Project leader for National and European work packages. She worked as Team leader for DSP algorithms Development and Prototyping. In 1999, she worked as leader of the "RF and Mobile Applications Studies" group in the Domain of Cellular, WLAN and WPAN embedded applications. Since 2004, the group activity has included studies on Software Radio, then Cognitive Radio with emphasis on optimising power consumption and evaluating complexity.



**Branka Vucetic** (M'83-SM'00-F'03) received the B.S.E.E., M.S.E.E., and Ph.D. degrees in 1972, 1978, and 1982, respectively, in electrical engineering, from The University of Belgrade, Belgrade, Yugoslavia. During her career she has held various research and academic positions in Yugoslavia, Australia, and the UK. Since 1986, she has been with the Sydney University School of Electrical and Information Engineering in Sydney, Australia. She is currently the Director of The Telecommunications Laboratory at Sydney University. Her research

interests include wireless communications, digital communication theory, coding, and multi-user detection. In the past decade she has been working on a number of industry sponsored projects in wireless communications and mobile Internet. She has taught a wide range of undergraduate, postgraduate, and continuing education courses worldwide. Prof. Vucetic co-authored four books and more than two hundred papers in telecommunications journals and conference proceedings.



**Dominique Barthel** graduated from Ecole Polytechnique and Ecole Supérieure d'Electricité in France. After a first career devoted to architecture and design of microprocessors, DSPs, mediaprocessors and scientific computers, his interest evolved to networked smart devices and sensor networks, with an emphasis on low power architectures and implementations. He currently leads the France Telecom research project on "technologies for mobile terminals and embedded devices". He holds six patents and is a devoted radio-amateur.